Hypertension Research (2018) 41:817–827
https://doi.org/10.1038/s41440-018-0090-9

ARTICLE

Hypertension-induced cognitive impairment: insights from prolonged angiotensin II infusion in mice

Sébastien Foulquier[1,2,3] · Pawel Namsolleck[2] · Britt T. Van Hagen[3,4] · Irina Milanova[1,2] · Mark J. Post[2,5] · W. Matthijs Blankesteijn[1,2] · Bart P. Rutten[3,4] · Jos Prickaerts[3,4] · Robert J. Van Oostenbrugge[2,3,6] · Thomas Unger[2]

Received: 15 December 2017 / Revised: 23 February 2018 / Accepted: 25 March 2018 / Published online: 17 August 2018

Abstract

The causal relation between hypertension and cerebral small vessel disease (cSVD) remains elusive, and appropriate animal models are scarce. We aimed to assess the relevance of prolonged angiotensin II-induced hypertension in mice for the study of cSVD.

Adult male C57BL/6 mice were continuously infused for 3 months with Angiotensin II (Ang II; 2 µg/kg/min, sc) or saline (control) via osmotic minipumps. Blood pressure, neurological function, locomotor activity, and working memory (Y-maze alternation task) were assessed throughout the study. Short-term memory performance (object location task) was measured after 3 months of infusion. Blood–brain barrier (BBB) function was assessed by the presence of IgG leakage and quantified in each brain area of interest. Microglial activation and myelin loss were studied in the areas of leakage.

Systolic blood pressure increased and remained elevated over the 3 months of Ang II infusion, while neurological scores and locomotor activity did not change. Working memory performance was also not changed, yet short-term memory performance was impaired in Ang II-treated mice compared to controls. While BBB leakages were present in both groups, mainly in the neocortex, hippocampus, and cerebral nuclei, Ang II-treated mice showed greater leakage than control mice, along with greater microglial density and soma size. Myelin loss was observed for the largest leaks.

Prolonged Ang II-induced hypertension is associated with large BBB leaks, microglial activation, myelin loss, and memory dysfunction in the absence of stroke.

Introduction

Cognitive impairment and dementia are major disabilities. The incidence rates of both are increasing due to population aging [1]. The vascular contribution to the pathophysiology of cognitive impairment has led to the concept of vascular cognitive impairment (VCI), which encompasses all cognitive disorders associated with cerebrovascular disease, from mild cognitive impairment to frank dementia [2, 3]. Age-related and vascular risk factor-related cerebral small vessel disease are probably the most prevalent causes of VCI. Hypertension is considered a major risk factor for the development of cerebral small vessel disease (cSVD) [4, 5]. Meta-analyzis of studies on hypertensive patients with left ventricular hypertrophy has revealed a twofold risk of cognitive impairment [6]. However, the contribution of hypertension to the pathological mechanism of cSVD remains elusive.

A recent review described all mouse models relevant to the study of cardiovascular risk factors on brain structure and cognition [7]. This review concluded that, although

Electronic supplementary material The online version of this article (https://doi.org/10.1038/s41440-018-0090-9) contains supplementary material, which is available to authorized users.

✉ Sébastien Foulquier
s.foulquier@maastrichtuniversity.nl

1 Department of Pharmacology-Toxicology, Maastricht University, Maastricht, The Netherlands

2 CARIM, School for Cardiovascular Diseases, Maastricht University, Maastricht, The Netherlands

3 MHeNS, School for Mental Health and Neuroscience, Maastricht University, Maastricht, The Netherlands

4 Department of Psychiatry and Neuropsychology, Maastricht University, Maastricht, The Netherlands

5 Department of Physiology, Maastricht University, Maastricht, The Netherlands

6 Department of Neurology, Maastricht University Medical Center +, Maastricht, The Netherlands

hypertension is considered the most important cause of cerebrovascular disease, mouse models of chronic hypertension are scarce, and there is a strong need to characterize those models in terms of cognitive function [7].

Apart from mice, hypertensive rats – spontaneously hypertensive rats (SHR) and stroke-prone SHRs (SHR-SP) – are well-described hypertensive models of cSVD [8–11]. However, cognitive testing and interpretation of cognitive performance is difficult in these models as both strains exhibit behavioral features of attention-deficit/hyperactivity disorder [12–14]. Additionally, for studies of the impact of hypertension on cognitive function, the control group should be of the same strain as the experimental group, which is not feasible with this model. The traditional use of Wistar-Kyoto rats (WKY) as the normotensive control for SHR and SHR-SP has been a matter of debate for decades due to their biological variability [15, 16]. It has been shown in several studies that young and aged WKY exhibit similar or worse cognitive scores than SHR and much worse scores than Sprague Dawley rats, another normotensive rat model [12, 17, 18].

In this context, the use of the Ang II infusion model appears to be a good alternative for the study of hypertension-induced cognitive dysfunction, since the same mouse strain is used in the normotensive and hypertensive groups. This ensures the absence of potential adaptation during development due to the characteristic genetic defects in genetic models of hypertension. This model also has another advantage in that minipumps can be implanted in a variety of other mouse models (disease, transgenic, and reporter). Previous studies that administered Ang II either acutely (1–4 days) or subchronically (3–4 weeks) at a standard dose (1 µg/kg/min) did not reveal any cognitive dysfunction in adult mice [19]. However, with the use of a higher dose of Ang II that induces malignant hypertension (1.9 µg/kg/min), differences in learning abilities were found, albeit only after 3 weeks of infusion [20]. The aim of the present study was to assess the impact of a prolonged high-dose Ang II infusion on BBB integrity and neuroinflammation and to determine its relevance to the study of hypertension-related VCI.

Methods

Animals

The study was performed using 20 adult male C57BL/6 mice (Charles River, Sulzfeld, Germany) that were 3–4 months old at the start of the experiments. The animals were housed individually on a reversed light/dark cycle (lights on from 7:00 PM to 7:00 AM), with food and water available ad libitum. The mice were allowed to habituate to the environment for 2 weeks prior to the start of experiment. The mice were weighed weekly. The animal experiments were approved by the regulatory authority of Maastricht University and were performed in compliance with the national and European guidelines.

Angiotensin II infusion and blood pressure measurement

Mice were infused with Ang II (2 µg/kg/min; Ang II; $n = 10$) or saline (control; $n = 10$) subcutaneously via osmotic minipumps (Alzet model 1004, Durect Corp., Cupertino, CA, USA). The minipumps were replaced every 4 weeks to maintain perfusion over 3 months. Three deaths were observed in the Ang II group due to hemorrhage in the ribcage. Systemic blood pressure was measured every 1–2 weeks throughout the 3-month period with a tail cuff (CODA, Kent Scientific) [21]. The mice were placed into a restraint device and placed on a warming platform. The animals were allowed to acclimate to the holder for 15 min before the start of the measurement. Each recording session consisted of 30 inflation–deflation cycles per set.

Behavioral tests

All behavioral testing was performed during the dark period of the light/dark cycle under dim lighting conditions. The Garcia neurological test was conducted weekly to assess motor and behavioral deficits indicative of major neurological damage such as stroke. In this composite neurological examination, 6 tests were used to provide an overall score on a scale from 0 to 18 points. To assess cognitive functioning, we used the Y-maze spontaneous alternation task and object location task (OLT) to measure working memory and short-term memory, respectively.

Spatial working memory was assessed with the Y-maze spontaneous alternation task [22]. Briefly, each mouse was placed in a randomly selected starting arm of a Y-maze and allowed to freely explore the arena for 6 min. The number of arm entries and the locomotor activity were recorded for each mouse using EthoVision (Noldus, Wageningen, The Netherlands). A successful alternation, designated a “triad”, was made if the mouse visited all 3 arms of the maze consecutively. The alternation percentage was calculated as the number of triads divided by the maximum possible number of alternations per mouse (total number of arm entries $- 2) \times 100$. An alternation rate above 50% (the chance-level probability of choosing the unfamiliar arm) is indicative of a functional working memory.

Short-term spatial memory was tested using an OLT with a 1 h intertrial interval [22]. Briefly, this 2-trial task consisted of a learning (T1) trial and a test trial (T2). In T1, a set of two identical objects were placed symmetrically in the middle of a

circular arena, which the mouse was allowed to explore freely for 4 min. After a 1 h interval spent in their home cage, the mice were placed in the arena for T2; in this trial, which lasted 4 min, one of the objects (right or left) was moved to a different location (front or back), while all other stimuli were kept the same. As rodents are naturally curious, they will spend more time exploring the moved object than the stationary object if they remember the previous location. The time spent exploring each object was scored manually on a computer by an experimenter blind to the experimental groups. Before the testing session, animals were habituated to the empty arena and all objects and testing procedures for a period of 1 week. Four different sets of objects were used, and both the relocated object and its new location were varied; these variables were randomized in a balanced manner across groups and sessions to reduce any potential bias due to preference for a particular object or location. Exploration behavior and outcome measurements have been previously defined [22]. The discrimination index d2 assesses whether the mouse spends more time at the novel location than at the familiar location (the difference between location exploration times divided by the total exploration time). Functional spatial short-term memory is reflected by a d2 index higher than zero (both objects equally explored) [22].

Tissue isolation

Mice were terminally anesthetized with pentobarbital (150 mg/kg, I.P.). During sacrifice, blood was withdrawn from the vena cava and collected into a tube precoated with EDTA; the blood was then centrifuged at 1500 × *g*, 4 °C, for 10 min to isolate plasma. Plasma was stored at −80 °C prior to use. The animals were perfused intracardially with Tyrode's buffer followed by PFA 4% for 12 min at constant pressure. Eyeballs were harvested for the isolation of retinas as previously described [23]. The retinas were immersed in PFA 4% for 1 h and transferred to PBS with sodium azide until staining. Brains were collected at the same time, immersed in PFA 4% overnight, and transferred to PBS with sodium azide before slicing.

Immunohistochemistry

Brains were sliced coronally on a vibratome to a thickness of 50 µm and stained using the free-floating section technique. For each immunohistochemical staining, 10 slices per brain, representative of the whole brains, were stained and analyzed. A first series of brain slices was stained with a rabbit anti-collagen IV antibody (1:500, overnight 4 °C, Abcam 6586) and subsequently incubated with an Alexa Fluor 488-conjugated donkey anti-rabbit antibody (1:400, 2 h RT, Thermo Fisher A21206) for vascular quantification. A second series of brain slices was stained with an antibody against IgG (Biotin SP AffiniPure Donkey Anti-Mouse IgG, 1:100, overnight, 4 °C, Jackson ImmunoResearch 715-065-151) followed by an incubation with an Alexa Fluor® 647-streptavidin conjugate (1:400, 1 h 30 min RT, Thermo Fisher S32357) to assess the size and distribution of BBB leakages. Simultaneously, a BrainStain Imaging Kit (1:300, 30 min RT, Thermo Fisher B34650) containing FluoroMyelin, NeuroTrace Nissl stain and DAPI was used for better characterization of brain sections corresponding to BBB leakages. A third series of brain slices was stained with an antibody against microglia and macrophages (anti-Iba1 rabbit antibody, 1:1000, overnight 4 °C, Wako 019-19741) by means of the ABC technique. Immunostaining was developed by adding DAB solution to the brain slices. A fourth series of brain slices was costained for IgG (donkey anti-mouse IgG-AF488, 1:200, overnight 4 °C, Thermo Fisher A21202) and myelin basic protein (MBP) (rat anti-MBP, 1:500, overnight 4 °C, Millipore MAB386). The anti-MBP antibody was revealed by incubation with a secondary donkey anti-rat antibody coupled to biotin (1:400, 1 h 30 min RT, Jackson Immunoresearch 712-065-150) followed by an incubation with an Alexa Fluor® 594-streptavidin conjugate (1:500, 1 h 30 min RT, Thermo Fisher S-11227). Before each antibody incubation, the slices were washed in TBS-T, TBS, and TBS-T sequentially. Flat-mounted retinas were stained with Alexa Fluor 488-conjugated isolectin GS-IB4 (from *Griffonia simplicifolia*, Thermo Fisher I21411, 20 µg/mL, overnight, 4 °C) to visualize the retinal vasculature.

CNS vasculature

The vasculature was analyzed in the cerebral cortex, the hippocampus and the thalamus using anti-collagen IV staining. Two brain slices were assessed per animal, and two z-stacks of 20 µm were analyzed per slice and per area. As the retinal vasculature is considered a clinically relevant vascular bed for the study of the brain vasculature, two retinal layers (the nerve fiber layer and the intermediate plexiform layer) were also analyzed using the same protocol (Supplementary Figure 2). Vascular density and junctions were assessed by using a semiautomatic analyzis tool (AngioTool) [24]. The following parameters were applied for the automatic analyzes: diameter, 5–10; intensity, 35–255; remove small particles, 40; fill holes, 200 (for collagen IV-positive vessels); diameter, 2–7; intensity, 50–255; remove small particles, 40; fill holes, 200 (for isolectin B4-positive vessels).

Analyzes of IgG leakages, microglia, and myelin integrity

Identification of IgG leakages was performed morphometrically by one investigator, who was blinded to the

experimental groups. IgG leakage was defined as a signal with an intense core and diffuse borders. All IgG leakages were listed for each brain area (PFC, prefrontal cortex encompassing the anterior cingulate area, the prelimbic area and the infralimbic area; CX, neocortex; HIPP, hippocampus; THAL, thalamus; CN, cerebral nuclei – defined by Allen's brain Atlas as encompassing the dorsal striatum, ventral striatum, septum and amygdala nuclei). The fluorescent signal of each leakage was then analyzed in ImageJ to quantify the leakage size in mm^2.

For the analyzis of microglial density and microglial soma size, two ROIs of 200 × 200 µm were analyzed per brain area per mouse. Each ROI was inverted in ImageJ before being processed with WIS-NeuroMath software [25]. The following parameters were applied for the automatic analyzes: noise level, 5; measure level, cell morphology; segmentation type, threshold; minimal cell intensity, 90; minimal area, 20; maximal area, 3850; minimal diameter, 4; maximal axial ratio, 8; minimal neurite length, 5.

The corpus callosum, a myelin-rich area, was used to assess potential changes in myelin composition due to hypertension. Corpus callosum thickness and MBP signal intensity were measured at 3 defined locations in the medial corpus callosum (bregma level: + 0.7 mm). The intensity of the myelin signal was further examined in IgG-positive areas (MBP_{IgG+}) versus IgG-negative areas (MBP_{IgG-}). Image stacks ($x = 550$; $y = 550$; $z = 30$ µm) of leakages were acquired by confocal microscopy (Leica TCS SPE). Maximum intensity projections of the IgG (Alexa Fluor 488) and MBP (Alexa Fluor 594) channels were generated in ImageJ. The change in myelin signal intensity $[(MBP_{IgG+})-(MBP_{IgG-})]/(MBP_{IgG-})$ was compared between small to middle-sized leakages (<0.05 mm^2) and large to very large leakages (>0.05 mm^2).

Chemicals

All chemicals were from Sigma-Aldrich (St. Louis, Missouri, USA) unless otherwise specified.

Statistical analyzes

Data were analyzed by the researchers in a blinded manner. All data are presented as the mean and standard error of the mean (SEM). Two-way analyzis of variance (ANOVA) was performed to compare the interaction and the effects of groups (control and Ang II) and time or brain areas (Systolic Blood Pressure (SBP), locomotor activity, working memory, cumulative latency, vascular density, junction density, microglial density, microglial soma). Sidak's correction was applied to post hoc multiple comparisons. *t*-tests were used to evaluate the effect of group on total exploration time, index discrimination d2, vascular density, number of junctions, leakage density, average leak size, and change in myelin signal. As indications for memory performance, the Y-maze spontaneous alternation test (alternation rate %) and the OLT (d2 index) were also subjected to one-sample *t*-tests, with testing values set at chance levels of 50 and 0, respectively. Statistical significance was defined by an alpha of 0.05, and all tests were two-tailed. All statistical analyzes were conducted using GraphPad Prism (GraphPad Software, San Diego, CA, USA).

Results

Body weight, blood pressure, behavior, and cognitive function

Body weight was decreased by Ang II infusion and reached 26.7 ± 0.7 g in the Ang II group and 29.0 ± 0.4 g in the control group at week 12 (Fig. 1a, $p_{AngII} < 0.05$). Systolic blood pressure increased following Ang II infusion and reached a plateau above 190 mmHg after 4 weeks of infusion; this plateau was maintained until the end of the study (Fig. 1b, $p_{AngII} < 0.05$). Neurological scores did not change throughout the whole study (Garcia scores, Supplementary Figure 1), and locomotor activity was not impaired by the Ang II infusion (Fig. 1c, $p = 0.25$).

The alternation rate was significantly above the chance level in the control group and remained unchanged in the Ang II group (Fig. 2a). In the object location task, the total exploration time of both objects in T2 was similar in both groups (Fig. 2b). However, the discrimination index d2 differed significantly from zero in the control group, while it was not different from zero in the Ang II group, which tended to differ from the control group (Fig. 2c).

CNS vascular density

Vascular density and junction density were slightly but significantly decreased by Ang II in all areas ($p_{AngII} < 0.05$), but post hoc analyzes did not reveal significant decreases in the cortex, the hippocampus or the thalamus (Fig. 3). Density was significantly decreased in both the nerve fiber layer and the intermediate plexiform layer of the retina (Supplementary Figure 2).

Blood–brain barrier leakage

The number of leaks did not differ between the control and Ang II groups (Fig. 4b). However, the average size of IgG leaks was 30 times larger in the Ang II group than in the control group (Fig. 4a, c). The size distribution of IgG leaks revealed a shift from small and middle-sized leaks (0–0.01, 0.01–0.05 mm^2) in control mice to middle-sized, large, and very large leaks in Ang II mice (0.01–0.5, 0.05–0.2,

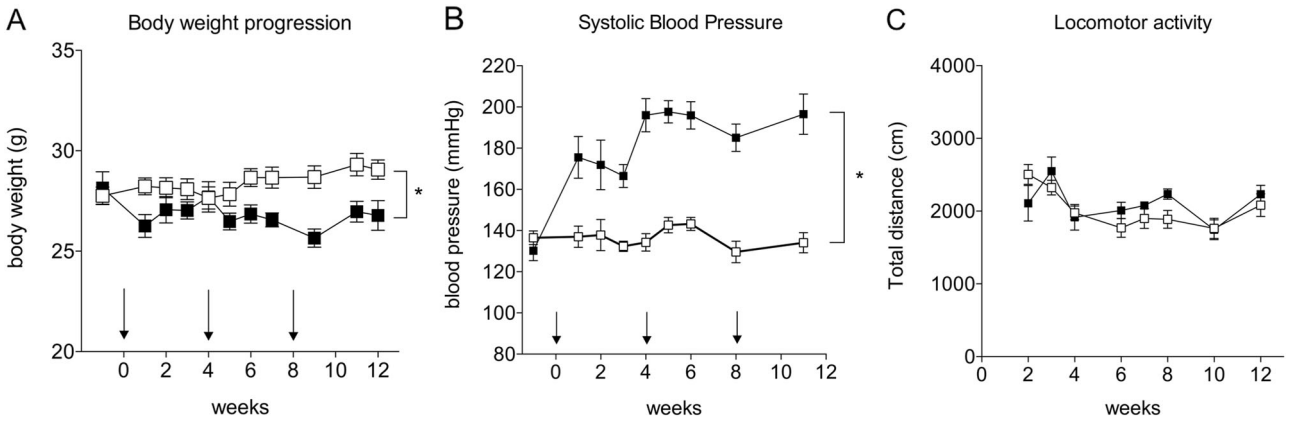

Fig. 1 Body weight, blood pressure, and locomotor activity. Progression of body weight (**a**), systolic blood pressure (**b**), and locomotor activities (**c**) over time in control (empty boxes) and Ang II mice (full boxes). Arrows indicate days of minipump implantation. $*p_{AngII} < 0.05$. $n = 7–10$ mice per group

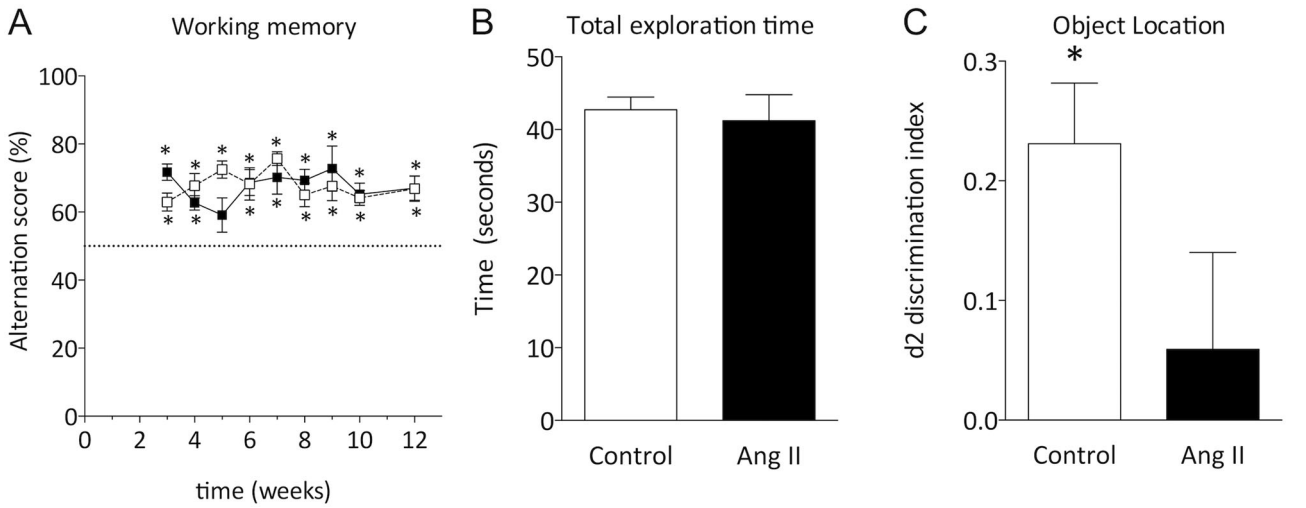

Fig. 2 Working and short-term memory performance progression of the alternation rate in the spontaneous Y-maze alternation task (**a**); total exploration time (**b**), and discrimination index d2 (**c**) in the object location task at 12 weeks. Ang II (full boxes/bars), control (empty boxes/bars). Significant differences from chance level as indicated by a one-sample t-test are indicated by an asterisk, $*p < 0.05$. $n = 7–10$ mice per group

>0.2 mm^2) (Fig. 4d). The observed leaks were localized in the prefrontal cortex, neocortex, hippocampus, cerebral nuclei, and thalamus. The average leak size was increased in the neocortex, the hippocampus and the cerebral nuclei of Ang II mice and differed significantly from the control in the cerebral nuclei (Fig. 4e, $p_{int} < 0.0001$, $p_{area} < 0.0001$, $p_{AngII} < 0.001$).

Microglial activation

There was an overall difference between the control and Ang II groups in microglial density (Fig. 5b, p_{int} 0.03, $p_{area} < 0.001$, $p_{AngII} < 0.0001$) as well as microglial soma size (Fig. 5c, p_{int} 0.42, $p_{area} < 0.001$, $p_{AngII} < 0.0001$). In the Ang II group, the microglial density was increased in the neocortex, hippocampus and thalamus (posttest, $p < 0.05$), and the soma size was increased in neocortex, hippocampus, and cerebral nuclei (posttest, $p < 0.05$).

Myelin integrity

Neither the size of the corpus callosum nor the intensity of the myelin signal was affected in the Ang II group (Fig. 6). Small and middle-sized leaks (0–0.05 mm^2) were not associated with decreased myelin signal, while large leaks (>0.05 mm^2) were found to be associated with a decrease (−29%, $p < 0.05$) in myelin content (Fig. 7).

Discussion

In the present study, we investigated the suitability of prolonged Ang II infusion as a way to mimic features of VCI. We showed that blood pressure remained high throughout the entire study, and we observed the presence of large BBB leaks accompanied by microglial activation in several brain

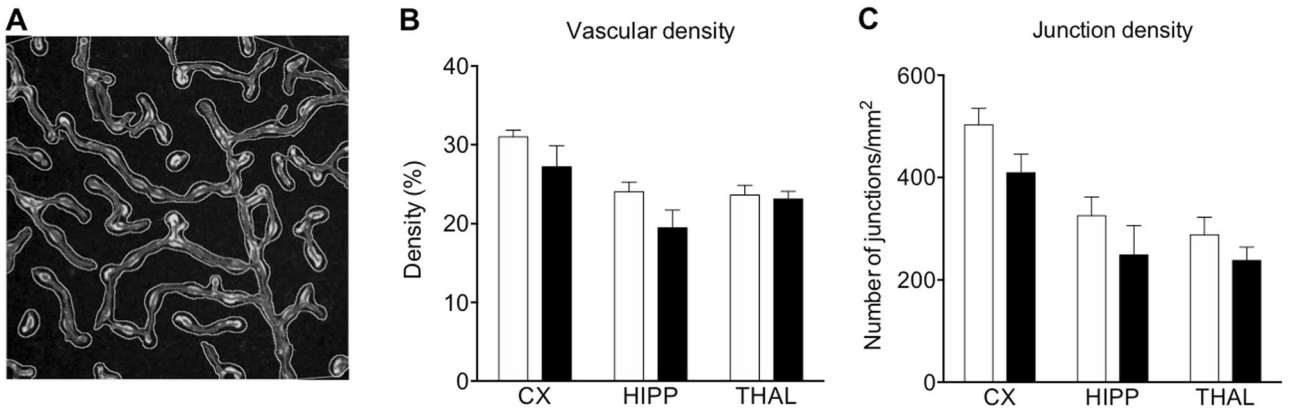

Fig. 3 Density of vessels and junction in the cerebral cortex, hippocampus, and thalamus. Vasculature stained for collagen IV (in green) was analyzed with AngioTool software. Representative image of the cortex (**a**); vascular density (%)in the control (empty bars) and Ang II groups (full bars) in each area of interest ($p_{int} = 0.38$; $p_{area} < 0.0001$; $p_{AngII} = 0.02$) (**b**); and junction density (number/mm^2) in each area of interest in the control (empty bars) and Ang II groups (full bars) ($p_{int} = 0.87$; $p_{area} < 0.0001$; $p_{AngII} = 0.04$) (**c**); CX neocortex, HIPP hippocampus, THAL thalamus; $n = 6$–10 mice per group

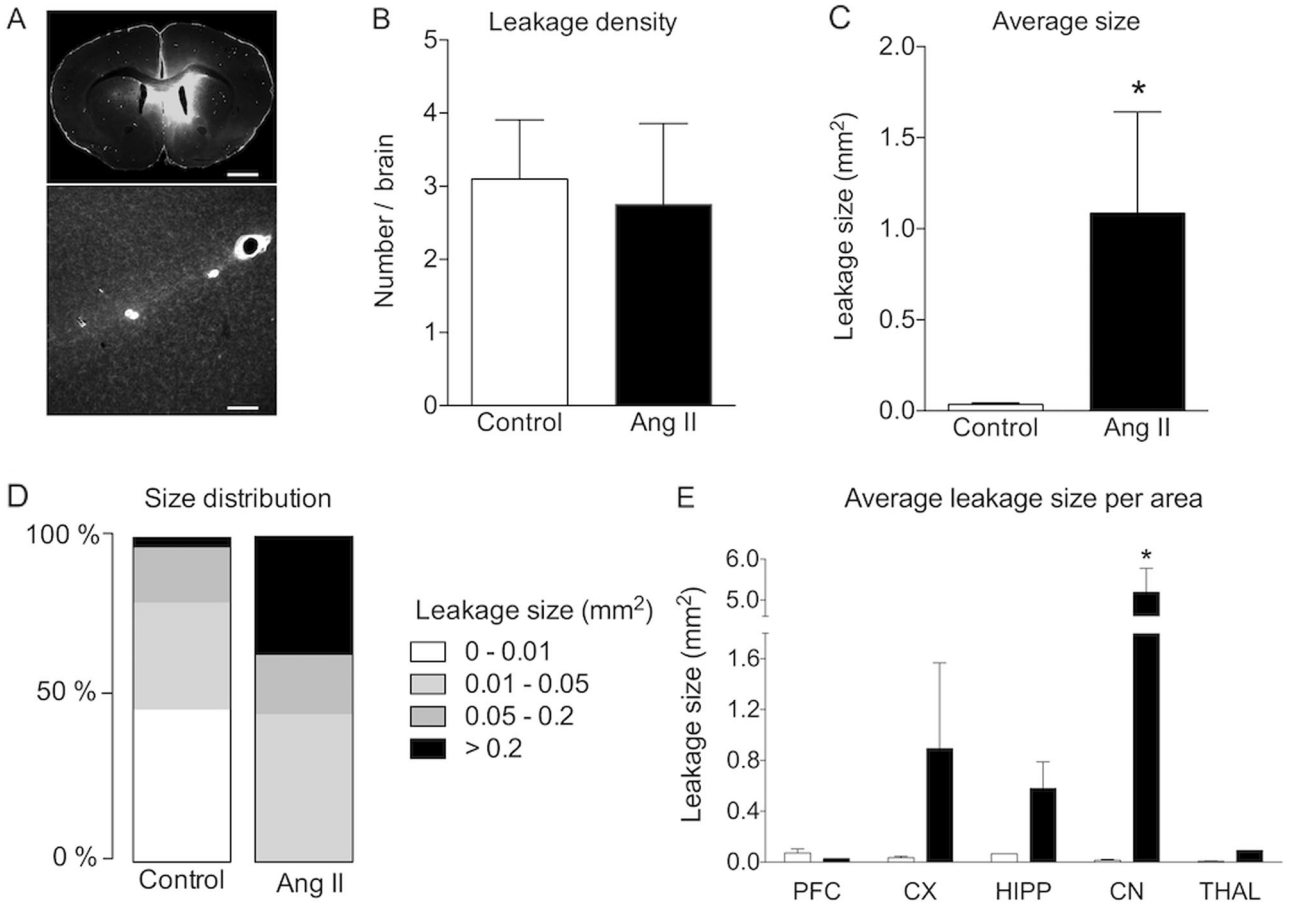

Fig. 4 Blood–brain barrier leakages. Leakages identified by IgG-positive staining in brain slices from control and Ang II mice. **a** Representative large (top, scale bar = 1 mm) and small leakages (bottom, scale bar = 150 µm); average leakage densities (**b**) and sizes (**c**) in control (empty bars) and Ang II mice (full bars); **d** size distribution of BBB leakages; **e** average leakage size in each brain area of interest. PFC prefrontal cortex, CX neocortex, HIPP hippocampus, CN cerebral nuclei, THAL thalamus. Multiple comparisons with Sidak correction, $^*p < 0.05$. $n = 7$–10 mice per group

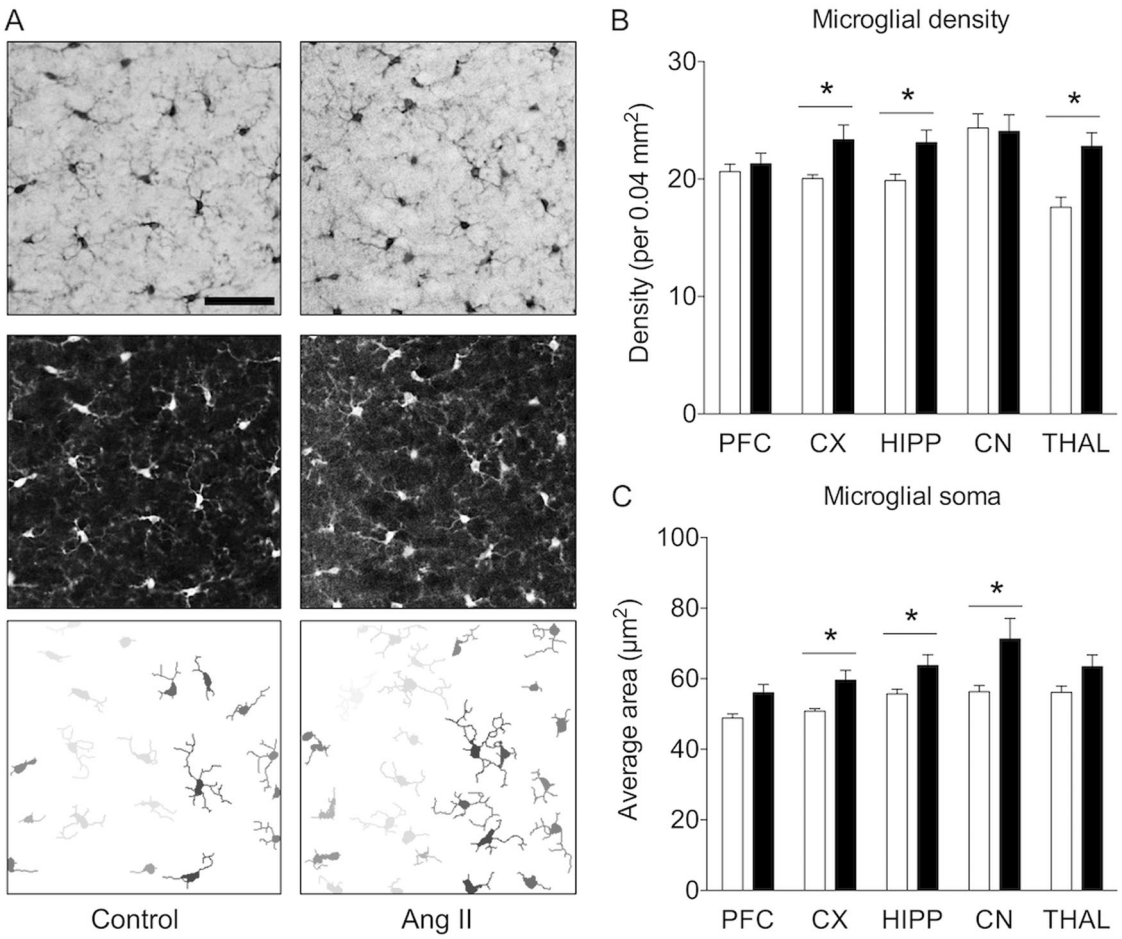

Fig. 5 Microglial activation. Representative pictures of Iba1-positive cells in cortical areas of control (**a**, left column) and Ang II mice (**a**, right column), in their raw state (**a**, upper row), after inversion (**a**, middle row) and automatic analyzes using WIS-NeuroMath software (**a**, bottom row) (scale bar = 50 µm). Microglial densities (**b**) and soma sizes (**c**) resulting from the automatic analyzis per brain area. PFC prefrontal cortex, CX neocortex, HIPP hippocampus, CN cerebral nuclei, THAL thalamus. Sidak's multiple comparisons posttest, $*p < 0.05$. $n = 7$–10 mice per group

areas, myelin loss for large leaks, and impairment of short-term memory. Both BBB leakage and microglial activation were evident mainly in the cerebral nuclei and the hippocampus, whereas the prefrontal cortex appeared to have been relatively spared in this respect. This suggests that the functional deficits found in the present study were related mainly to hippocampal and basal ganglia dysfunctions. Thus, the model only partly mimics human cSVD, in which cognitive decline is typically associated with lacunar infarcts or microbleeds in subcortical areas (basal ganglia and hemispheric white matter) [2, 26]. In the present model, microbleeds were not observed (May Grünwald Giemsa, data not shown).

While the cognitive function of young mice submitted to a 4-week Ang II infusion (1 µg/kg/min) was not impaired in a prior study [19], we were able to confirm this result only for working memory and not for short-term memory, which was impaired at 6 months of age after a prolonged infusion of Ang II. In addition to the duration of infusion, the increase in blood pressure was also greater in our study than in the previous one due to a higher dose of Ang II (Ang II group in the present study, SBP 196 mmHg; Ang II groups in Toth et al. [19], SBP ≈ 150 mmHg). In a recent study, authors have shown that mice that develop hypertension (2 weeks of Ang II infusion at 1 µg/kg/min + L-NAME treatment at 100 mg/kg BW) exhibited normal cognitive function during a novel object recognition task [27]. At 4 weeks of treatment, short-term memory in this model was decreased, while long-term memory was preserved. An additional daily Ang II bolus (0.5 µg/kg BW s.c.) from 2 weeks onwards led to impairment of both short- and long-term memory at 4 weeks. This highlights the possibility that Ang II infusion can be used to fine-tune the severity of the model depending on the dosage and duration of the infusion. In our model, the prolonged blood pressure elevation induced by Ang II resulted in a slight overall decrease in cerebral vascular and vascular junction densities. This

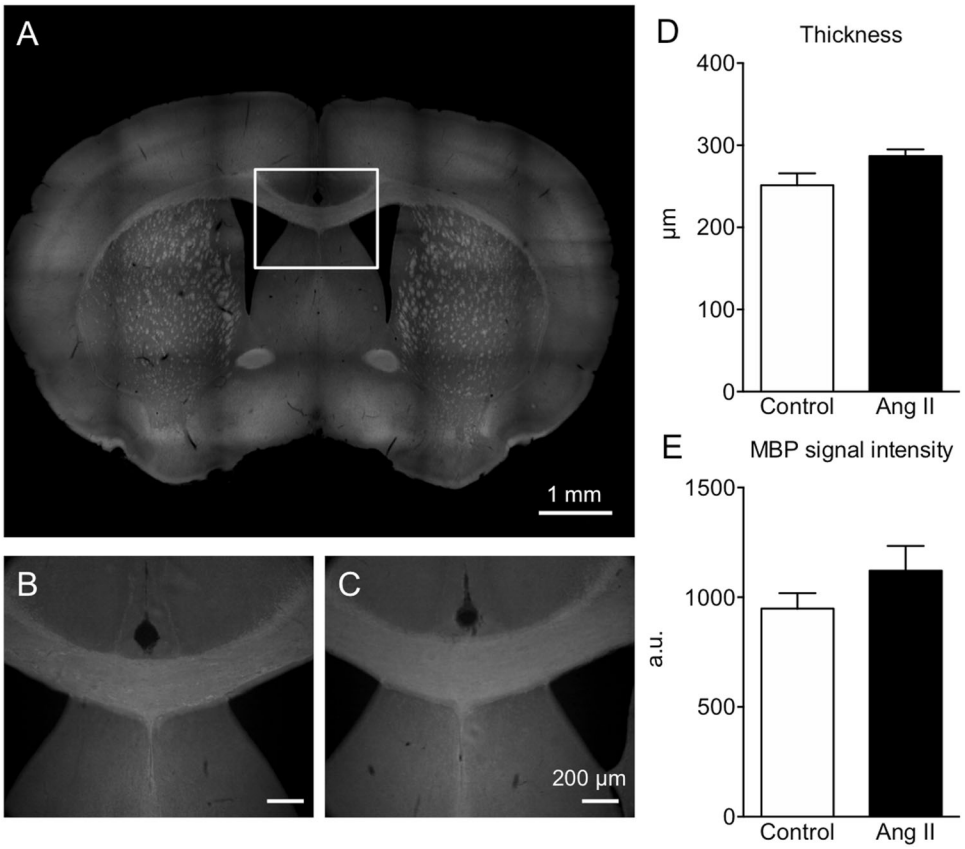

Fig. 6 Corpus callosum integrity. Representative image of myelin basic protein (MBP) staining (**a**: whole brain slice; **b**, **c**: medial corpus callosum in control and Ang II mice, respectively). **d** medial corpus callosum thickness; **e** MBP signal intensity in the medial corpus callosum. $n = 7$–10 mice per group

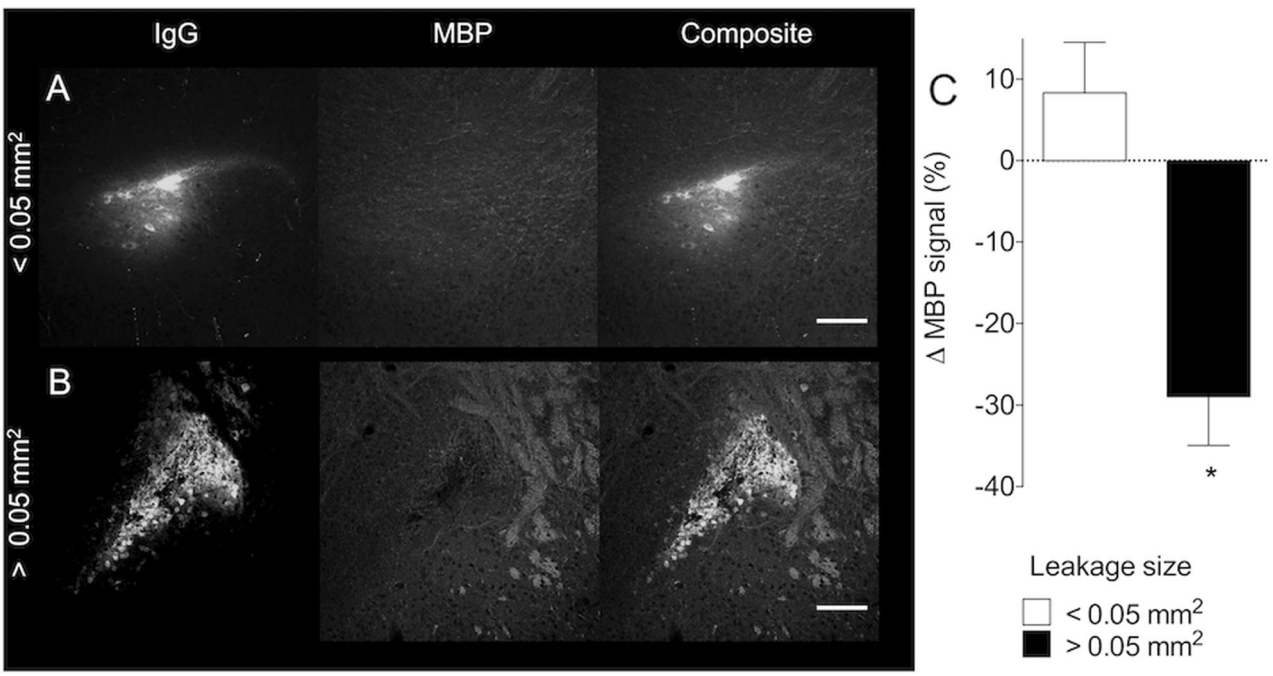

Fig. 7 Myelin content in BBB leakages Representative images of IgG and MBP staining from small/middle-sized leakages (row **a**, < 0.05 mm^2) and large/very large leakages (row **b**, > 0.05 mm^2). Left column: IgG staining (green). Middle column: MBP staining (red). Right column: composite image. (Scale bar = 100 µm.) **c** change in MBP signal in IgG$^+$ vs IgG$^-$ areas grouped by leakage size. t-test; *$p < 0.05$. $n = 7$–10 mice per group

effect, however, was not significant for individual areas as observed in other studies [28]. In the retina, a similar (but significant) decrease was observed in both layers (Supplementary Figure 2), highlighting the relevance of the retinal vasculature as an indicator of hypertension-induced cerebrovascular remodeling. Although our model consists of prolonged Ang II-induced hypertension, the duration of the blood pressure elevation may not be enough to lead to strong microvascular rarefaction (−10% in cortex, $p > 0.05$; −20% in hippocampus, $p > 0.05$; −2% in thalamus, $p > 0.05$). Another study has shown that aging in combination with short Ang II infusion (4 weeks) led to a similar decrease in capillary density (−10 to −20% in cortical and hippocampal areas) [19]. We suggest that our prolonged Ang II approach may therefore have a more profound effect in aged mice than in younger mice.

Our results show that plasma components, including IgG, penetrated into the brain through the damaged BBB (Fig. 4). Leakage of plasma components may lead to neuroinflammation and, subsequently, to neuronal dysfunction [29]. IgG can induce microglial activation by binding to IgG Fc receptors [30–32]. Further, our study provides evidence that, following hypertension, increased IgG leakage is associated with an exacerbated neuroinflammatory response as shown by the increased density and soma size of microglia in the cortex, hippocampus, cerebral nuclei, and thalamus (Fig. 5). In other Ang II models with shorter and more moderate blood pressure elevation, no microglial activation was observed [19, 28]. However, in aged Ang II-infused mice, BBB leakage, and microglial activation have been observed, suggesting age-dependent sensitivity of cerebral vessels to hypertension [19]. Microglial activation was also found in mice with short Ang II infusion, but in association with concomitant L-NAME treatment and Ang II bolus administration [33]. As in our study, microglial activation has also been found in deep cortical regions of SHR in association with albumin leakage [8], suggesting that the microglial activation observed is due to leakage resulting from hypertension rather than from Ang II itself.

Recent work has evidenced the major contribution of perivascular macrophages (PVMs) in Ang II-induced BBB dysfunction. PVMs are distinct from microglia, as they originate from hematopoietic precursors. They reside in the perivascular space and can react upon stimulation of angiotensin AT_1 receptors via the production of reactive oxygen species [34]. The detrimental role of PVMs has been confirmed in spontaneous hypertensive mice (BPH/2J) by showing a restoration of their cognitive function upon PVMs depletion [34]. Whether PVMs activation constitute the first step in the pathological cascade initiated by BBB disruption, relayed by microglial activation, needs to be determined.

In cSVD subjects, the presence of microglial activation remains to be investigated. A postmortem histological study in humans has revealed the presence of microglial activation in white matter lesions from aged brains [35]. As white matter lesions are features of both aging and cSVD, further studies on postmortem tissues from cSVD subjects are required to confirm this association. As reported in other studies with Ang II-infused models, the lack of apparent white matter lesions in mice might result from the limited duration of the Ang II infusion [33]. In our prolonged Ang II model, myelin loss was evidenced but was observed only in the presence of large leaks, while the corpus callosum, a myelin-rich area, was unaffected.

Limitations

Our chronic hypertensive model shares a key limitation with other Ang II infusion models: the limited clinical relevance due to the unifactorial etiology of Ang II-induced hypertension versus the multifactorial aspect of clinical hypertension. In addition, while adult mice (3–6 months old) were used in this study to gain first insights into the impact of a prolonged Ang II infusion, older mice (12–18 months old) may be more susceptible to BBB impairment and, as such, would increase the relevance of this model for the study of VCI. A second limitation of the present study is related to the presence of BBB leakage. Indeed, the microglial activation observed may result not only from the presence of plasma components that triggered microglial activation but also from direct microglial activation mediated by Ang II leaked from the plasma, similarly to recent findings in PVMs. Furthermore, leakage of circulating Ang II may exert direct neuronal actions by binding different angiotensin receptors and thereby influence neuronal plasticity and memory consolidation [36–39].

Perspectives

Our study has revealed cognitive dysfunction in mice submitted to prolonged Ang II-induced hypertension. We also showed increased permeability of the BBB in these mice, echoing major pathophysiological pathways seen in human cSVD. Hypertension-mediated cognitive impairment was associated with a cerebrovascular density decline, BBB leakage, microglial activation and, less commonly, myelin loss. Future studies are needed to establish causal links among those pathological observations. In particular, longitudinal imaging studies and intervention studies are required to better decipher the exact pathological cascade taking place in this model. Furthermore, the addition of other risk factors to the present model, such as aging, diabetes, or atherosclerosis, would allow a better understanding

of the development of VCI and the identification of potential therapeutic targets to prevent or delay its progression. In absence of targeted therapy, efficient management of hypertension with an appropriate timing [40] remains the only preventive measure to reduce cerebrovascular risk.

Acknowledgements We are grateful to Wiel Honig, Geertje Seewnen, Hellen Steinbusch, Dr. Michal Bencze, and Dr. Chiara Recarti for their technical assistance; and to Prof. Harry Steinbusch for his advisory role.

Funding This work was partly supported by the 2015 ESH Servier Research grant on Hypertension. This project has received funding from the European Union's Horizon 2020 research and innovation program under grant agreement No. 666881, SVDs@target.

Compliance with ethical standards

Conflict of interest The authors declare that they have no conflict of interest.

References

1. World Health Organization, Alzheimer's Disease International. *WHO | Dementia: a public health priority*. http://www.who.int/mental_health/publications/dementia_report_2012/en/
2. Iadecola C. The pathobiology of vascular dementia. Neuron. 2013;80:844–66.
3. Gorelick PB, Scuteri A, Black SE, Decarli C, Greenberg SM, Iadecola C et al. Vascular contributions to cognitive impairment and dementia: a statement for healthcare professionals from theamerican heart association/american stroke association. Stroke. 2011;42:2672–713.
4. Iadecola C. Hypertension and dementia. Hypertension. 2014;64:3–5.
5. Pantoni L. Cerebral small vessel disease: from pathogenesis and clinical characteristics to therapeutic challenges. Lancet Neurol. 2010;9:689–701.
6. Georgakis MK, Synetos A, Mihas C, Karalexi MA, Tousoulis D, Seshadri S et al. Left ventricular hypertrophy in association with cognitive impairment: a systematic review and meta-analysis. Hypertens Res. 2017;40:696–709.
7. Bink DI, Ritz K, Aronica E, van der Weerd L, MJAP Daemen. Mouse models to study the effect of cardiovascular risk factors on brain structure and cognition. J Cereb Blood Flow Metab. 2013;33:1666–84.
8. Kaiser D, Weise G, Möller K, Scheibe J, Pösel C, Baasch S et al. Spontaneous white matter damage, cognitive decline and neuroinflammation in middle-aged hypertensive rats: an animal model of early-stage cerebral small vessel disease. Acta Neuropathol Commun. 2014;2:169.
9. Bailey EL, Wardlaw JM, Graham D, Dominiczak AF, Sudlow CLM, Smith C. Cerebral small vessel endothelial structural changes predate hypertension in stroke-prone spontaneously hypertensive rats: a blinded, controlled immunohistochemical study of 5- to 21-week-old rats. Neuropathol Appl Neurobiol. 2011;37:711–26.
10. Schreiber S, Bueche CZ, Garz C, Braun H. Blood brain barrier breakdown as the starting point of cerebral small vessel disease? - New insights from a rat model. Exp Transl Stroke Med. 2013;5:4.
11. Schreiber S, Bueche CZ, Garz C, Kropf S, Angenstein F, Goldschmidt J et al. The pathologic cascade of cerebrovascular lesions in SHRSP: is erythrocyte accumulation an early phase? J Cereb Blood Flow Metab. 2012;32:278–90.
12. Tayebati SK, Tomassoni D, Amenta F. Spontaneously hypertensive rat as a model of vascular brain disorder: microanatomy, neurochemistry and behavior. J Neurol Sci. 2012;322:241–9.
13. Sontag T-A, Fuermaier ABM, Hauser J, Kaunzinger I, Tucha O, Lange KW. Spatial memory in spontaneously hypertensive rats (SHR). PLoS ONE. 2013;8:e74660.
14. Ueno K, Togashi H, Mori K, Matsumoto M, Ohashi S, Hoshino A et al. Behavioural and pharmacological relevance of stroke-prone spontaneously hypertensive rats as an animal model of a developmental disorder. Behav Pharmacol. 2002;13:1–13.
15. Kurtz TW, Morris RC. Biological variability in Wistar-Kyoto rats. Implications for research with the spontaneously hypertensive rat. Hypertension. 1987;10:127–31.
16. H'Doubler PB, Peterson M, Shek W, Auchincloss H, Abbott WM, Orkin RW. Spontaneously hypertensive and Wistar Kyoto rats are genetically disparate. Lab Anim Sci. 1991;41:471–3.
17. Diana G. Does hypertension alone lead to cognitive decline in spontaneously hypertensive rats? Behav Brain Res. 2002;134:113–21.
18. Robertson B-A, Clements KM, Wainwright PE. The working memory capabilities of the spontaneously hypertensive rat. Physiol Behav. 2008;94:481–6.
19. Toth P, Tucsek Z, Sosnowska D, Gautam T, Mitschelen M, Tarantini S et al. Age-related autoregulatory dysfunction and cerebromicrovascular injury in mice with angiotensin II-induced hypertension. J Cereb Blood Flow Metab. 2013;33:1732–42.
20. Duchemin S, Belanger E, Wu R, Ferland G, Girouard H. Chronic perfusion of angiotensin II causes cognitive dysfunctions and anxiety in mice. Physiol Behav. 2013;109:63–8.
21. Daugherty A, Rateri D, Hong L, Balakrishnan A. Measuring blood pressure in mice using volume pressure recording, a tail-cuff method. *J Vis Exp*. 2009; 27: e1291.
22. Sierksma ASR, Prickaerts J, Chouliaras L, Rostamian S, Delbroek L, Rutten BPF et al. Behavioral and neurobiological effects of prenatal stress exposure in male and female APPswe/PS1dE9 mice. Neurobiol Aging. 2013;34:319–37.
23. Caolo V, Swennen G, Chalaris A, Wagenaar A, Verbruggen S, Rose-John S et al. ADAM10 and ADAM17 have opposite roles during sprouting angiogenesis. Angiogenesis. 2015;18:13–22.
24. Zudaire E, Gambardella L, Kurcz C, Vermeren S. A computational tool for quantitative analysis of vascular networks. PLoS ONE. 2011;6:e27385.
25. Rishal I, Golani O, Rajman M, Costa B, Ben-Yaakov K, Schoenmann Z et al. WIS-NeuroMath enables versatile high throughput analyses of neuronal processes. Dev Neurobiol. 2013;73:247–56.
26. Jellinger KA. Pathology and pathogenesis of vascular cognitive impairment-a critical update. Front Aging Neurosci. 2013;5:17.
27. Meissner A, Minnerup J, Soria G, Planas AM. Structural and functional brain alterations in a murine model of Angiotensin II-induced hypertension. J Neurochem. 2017;140:509–21.
28. Cifuentes D, Poittevin M, Dere E, Broquères-You D, Bonnin P, Benessiano J et al. Hypertension accelerates the progression of Alzheimer-like pathology in a mouse model of the disease. Hypertension. 2015;65:218–24.
29. Zlokovic BV. The blood-brain barrier in health and chronic neurodegenerative disorders. Neuron. 2008;57:178–201.
30. Fuller JP, Stavenhagen JB, Teeling JL. New roles for Fc receptors in neurodegeneration-the impact on Immunotherapy for Alzheimer's Disease. Front Neurosci. 2014;8:235.

31. Vedeler C, Ulvestad E, Grundt I, Conti G, Nyland H, Matre R et al. Fc receptor for IgG (FcR) on rat microglia. J Neuroimmunol. 1994;49:19–24.
32. Komine-Kobayashi M, Chou N, Mochizuki H, Nakao A, Mizuno Y, Urabe T. Dual role of Fcgamma receptor in transient focal cerebral ischemia in mice. Stroke. 2004;35:958–63.
33. Meissner A, Minnerup J, Soria Rodriguez G, Planas AM Structural and functional brain alterations in a murine model of Angiotensin II - induced hypertension. J *Neurochem.* 2017; 140:509–21.
34. Faraco G, Sugiyama Y, Lane D, Garcia-Bonilla L, Chang H, Santisteban MM et al. Perivascular macrophages mediate the neurovascular and cognitive dysfunction associated with hypertension. J Clin Invest. 2016;126:4674–89.
35. Simpson JE, Ince PG, Higham CE, Gelsthorpe CH, Fernando MS, Matthews F et al. Microglial activation in white matter lesions and nonlesional white matter of ageing brains. Neuropathol Appl Neurobiol. 2007;33:670–83. MRC Cognitive Function and Ageing Neuropathology Study Group
36. Tucsek Z, Noa Valcarcel-Ares M, Tarantini S, Yabluchanskiy A, Fülöp G, Gautam T et al. Hypertension-induced synapse loss and impairment in synaptic plasticity in the mouse hippocampus mimics the aging phenotype: implications for the pathogenesis of vascular cognitive impairment. *Geroscience* 2017;39: 385-406.
37. Gard PR. The role of angiotensin II in cognition and behaviour. Eur J Pharmacol. 2002;438:1–14.
38. Foulquier S, Steckelings UM, Unger T. Perspective: a tale of two receptors. Nature. 2013;493:S9.
39. Wright JW, Reichert JR, Davis CJ, Harding JW. Neural plasticity and the brain renin-angiotensin system. Neurosci Biobehav Rev. 2002;26:529–52.
40. Hermida RC, Ayala DE, Smolensky MH, Fernández JR, Mojón A, Portaluppi F. Chronotherapy with conventional blood pressure medications improves management of hypertension and reduces cardiovascular and stroke risks. Hypertens Res. 2016;39:277–92.